Supplementary Figures:

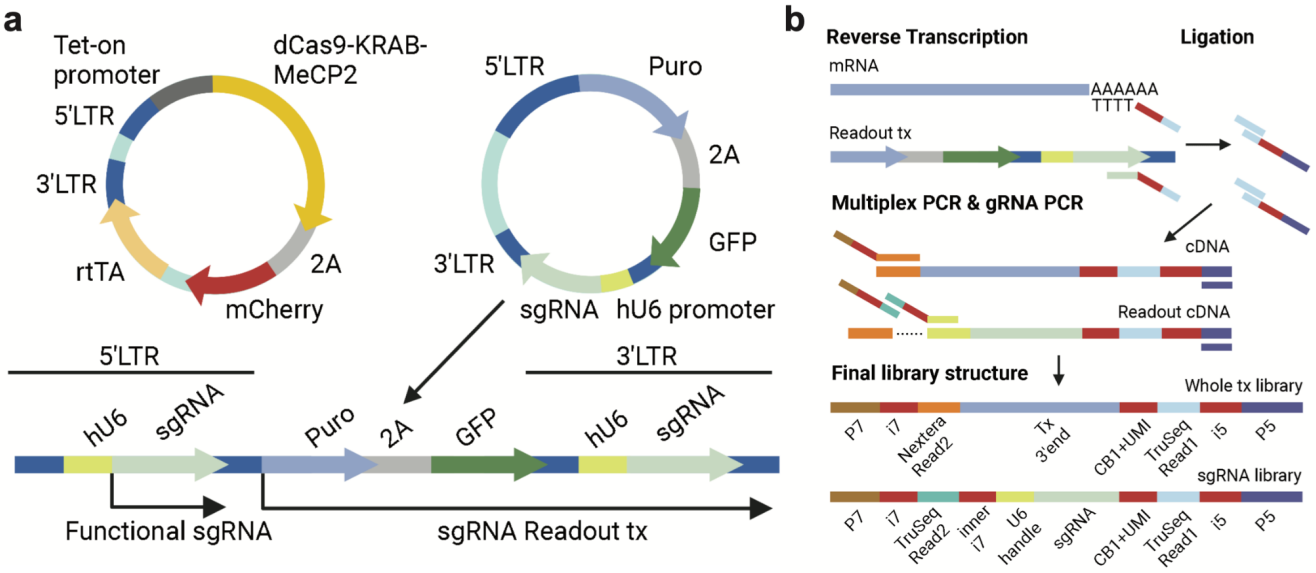

Extended Data Fig. 1. Scheme of plasmids and experiment procedures of *PerturbSci*. a. The vector system used in *PerturbSci* for dCas9 and sgRNA expression. The expression of the enhanced CRISPRi silencer dCas9-KRAB-MeCP2[11] was controlled by the tetracycline responsive (Tet-on) promoter. A GFP sequence was added to the original CROP-seq-opti plasmid[9] as an indicator of successful sgRNA transduction and for the lentivirus titer measurement. **b**. The library preparation scheme and the final library structures of *PerturbSci*, including a scalable combinatorial indexing strategy with direct sgRNA capture and enrichment that reduced the library preparation cost, enhanced the sensitivity of the sgRNA capture compared to the original CROP-seq[8], and avoided the extensive barcodes swapping detected in Perturb-seq[9].

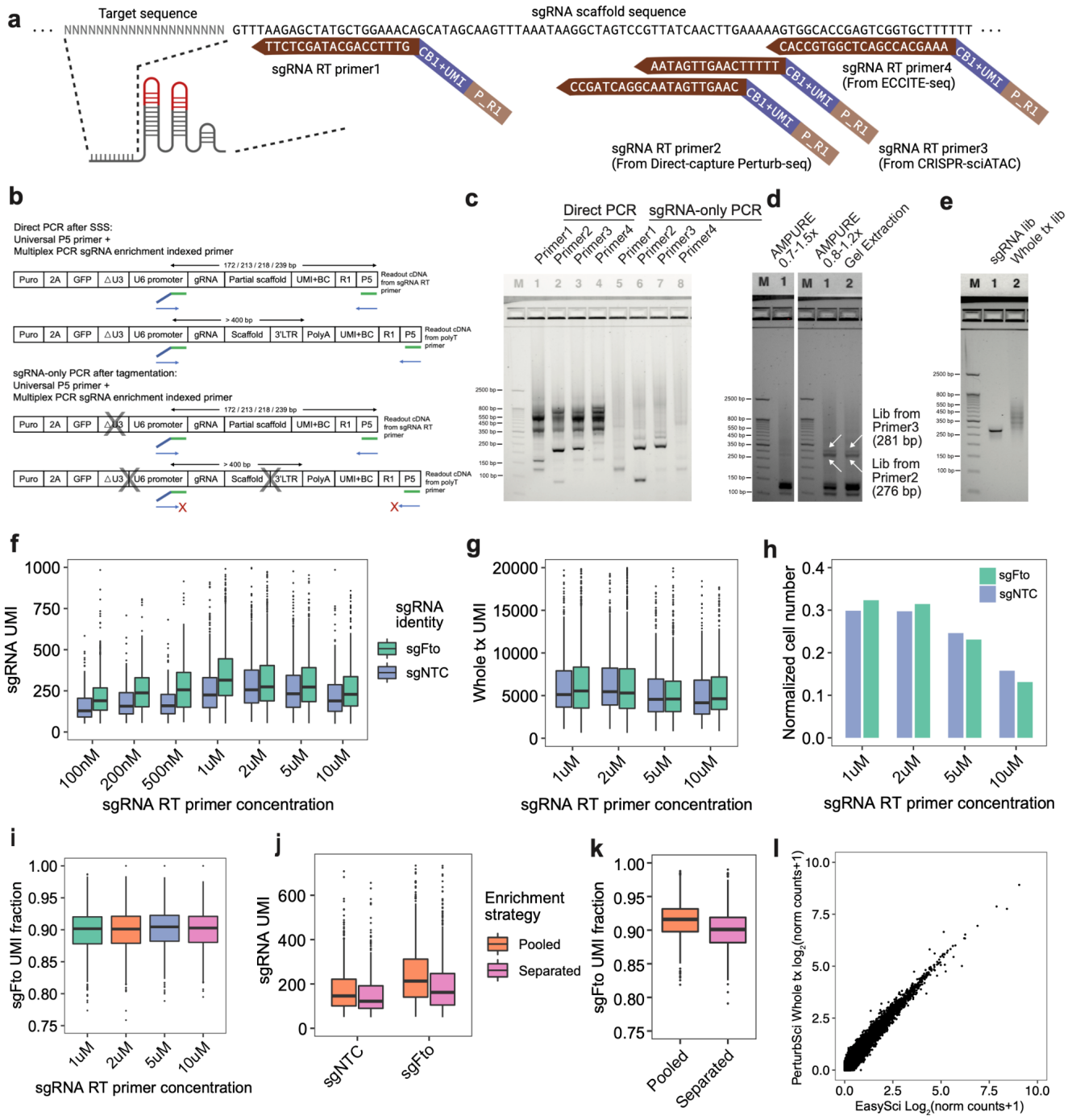

Extended Data Fig. 2. Representative optimizations on sgRNA enrichment of *PerturbSci*. a. Multiple RT primers targeting different sgRNA scaffold regions were mixed with polyT primers respectively and were used in our test experiment for targeted enrichment of sgRNA (RT primer 2-4 were modified from primers used in Direct-capture Perturb-seq[52], CRISPR-sciATAC[53], and ECCITE-seq[54]). CB, cell barcode. P_R1, partial TruSeq read1 sequence. **b-c.** A 96-well plate was divided into 4 parts and RT was performed

using different combinations of sgRNA capture primers and shortdT primers. After ligation, cells were mixed and redistributed for SSS. We tested the capture efficiency of sgRNA by different RT primers in *PerturbSci* using "Direct PCR" and tested the efficiency of by-product removal by "sgRNA-only PCR" (Scheme shown in b) followed by gel electrophoresis for analyzing the PCR product (c). Crosses in b, potential Tn5 tagmentation sites. As shown in c, sgRNA primer 2 and 3 yielded strongest amplification signals following PCR, while primer1 and 4 recovered weak signals. In addition, tagmentation removed large by-products generated potentially from polyT priming (as shown in b). **d.** We tested different conditions in post-multiplex PCR purification to obtain the input for the sgRNA enrichment PCR that could maximize the recovery of the sgRNA library. Left lane: 0.7x-1.5x double-size AMPURE beads purification followed by the sgRNA enrichment PCR reaction. Middle lane: 0.8x-1.2x AMPURE beads purification followed by the sgRNA enrichment PCR reaction. Right lane: Gel extraction on multiplex PCR product within 175-275 bp range followed by the sgRNA enrichment PCR reaction. The recovered sgRNA libraries generated from gRNA primer2 and 3 were marked on the gel image. Based on the result, the sgRNA primer2 and the 0.8-1.2x AMPURE beads purification condition yielded the best performance. **e.** A representative gel image of the final libraries of *PerturbSci*, including the sgRNA library (Lane 1) and the whole transcriptome library (Lane 2). **f-i.** We tested different concentrations of sgRNA RT primers in the PerturbSci experiment using 3T3-L1-CRISPRi cells transduced with either sgFto and sgNTC. The box plots show the number of unique sgRNA transcripts (f) or mRNA transcripts (g) detected per cell, the cell recovery rate (h) and sgRNA capture purity (i) across different sgRNA RT primer concentrations. **j-k.** We performed *PerturbSci* experiment with 3T3-L1-CRISPRi cells transduced with sgFto and sgNTC in a pooled or separate manner. The box plots show the number of unique sgRNA transcripts detected per cell (j) and sgRNA capture purity (k) across the two conditions. **l.** Scatter plot showing the correlation between log2-transformed aggregated gene expression profiled by *PerturbSci* and *EasySci*[10] in the mouse 3T3-L1-CRISPRi cell line.

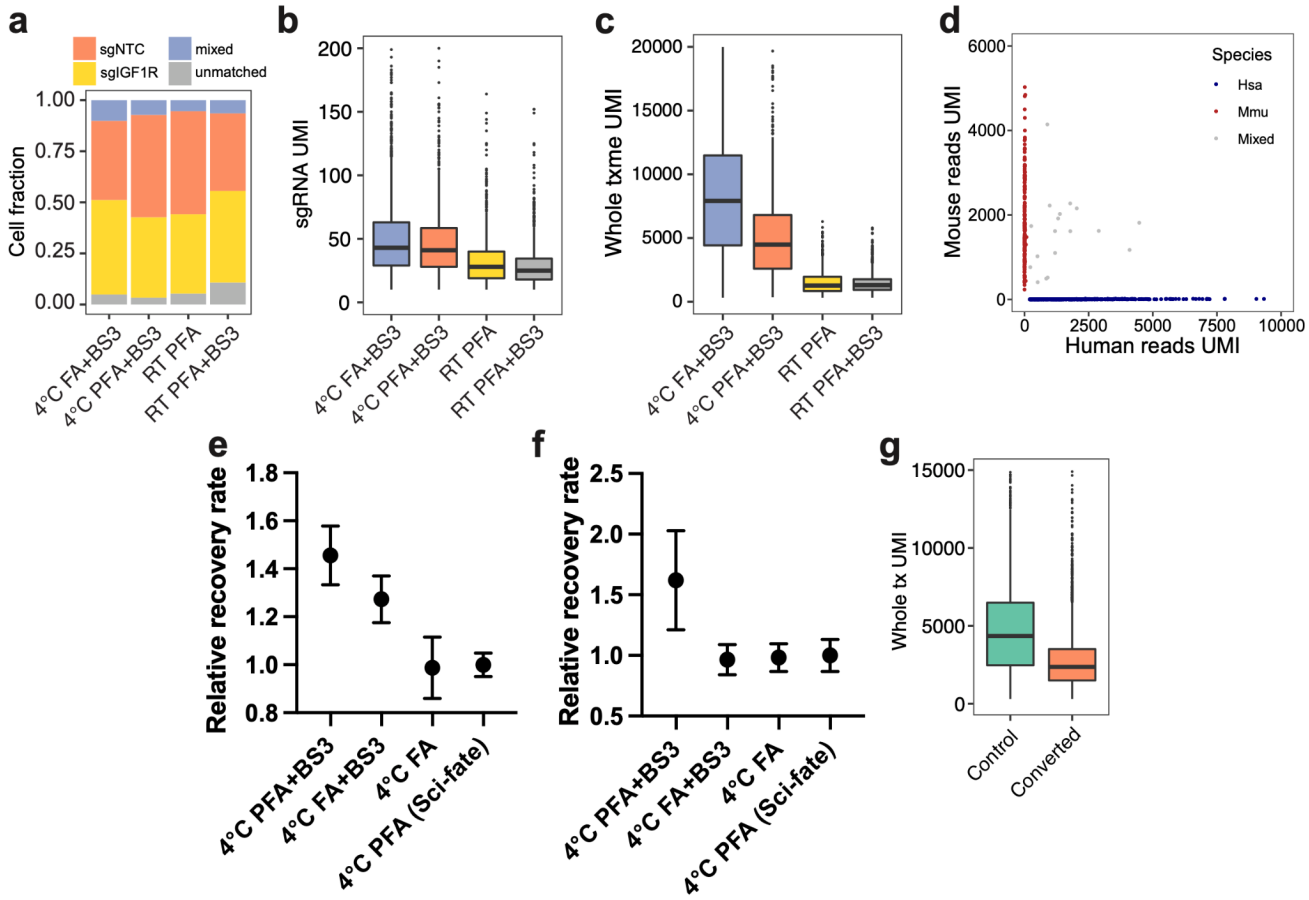

Extended Data Fig. 3. Representative optimizations on fixation conditions of *PerturbSci-Kinetics*. We aimed to search for an optimal fixation condition that can i) minimize the cell loss during the fixation and chemical conversion, ii) reduce the RNA cross-contamination, iii) be compatible with *in-situ* combinatorial indexing of cellular transcriptomes. **a-c.** We tested different cell fixation conditions on HEK293-idCas9 cells followed by *PerturbSci* profiling and quantified the fraction of cells that were assigned to different groups (a), the number of unique sgRNA (b) and mRNAs (c) detected per cell. PFA fixation conditions at the room temperature (RT) were too strong to recover sufficient signals. FA fixation at 4°C yielded higher total UMI counts but showed stronger cross-contamination, indicating that under 4°C it was a milder fixative compared to 4% PFA. **d.** Scatter plot showing the number of unique mRNA transcripts recovered from human HEK293-idCas9 cells and mouse 3T3 cells in a *PerturbSci* experiment. The human and mouse cell mixture was fixed by 4°C PFA+BS3 condition. Reads were aligned to a combined human-mouse reference genome and the species origins of single cells were identified by the fraction of species-specific read counts. The clear separation of cells from two species indicated the good

compatibility of this fixation condition with *PerturbSci*. **e-f.** Dot plots showing the relative recovery rate (with standard error of the mean) of HEK293-idCas9 cells in different fixation conditions (n = 4) following HCl permeabilization (d) and chemical conversion (e). All values were normalized by the standard condition used in sci-fate (PFA fixation)[14]. **g.** Box plot showing the number of unique transcripts detected per cell with or without chemical conversion. Fixation conditions included in the plots: 4°C PFA+BS3: cells were fixed with 4% PFA in PBS for 15 minutes, and were further fixed by 2mM BS3 during and after Triton-X100 permeabilization (**Methods**). 4°C FA+BS3: cells were fixed with 1% Formaldehyde (FA) in PBS for 10 minutes, and were further fixed by 2mM BS3 during and after Triton-X100 permeabilization. 4°C FA: cells were only fixed once with 1% Formaldehyde (FA) in PBS for 10 minutes. 4°C PFA: cells were only fixed once with 4% PFA in PBS for 15 minutes as sci-fate[14].

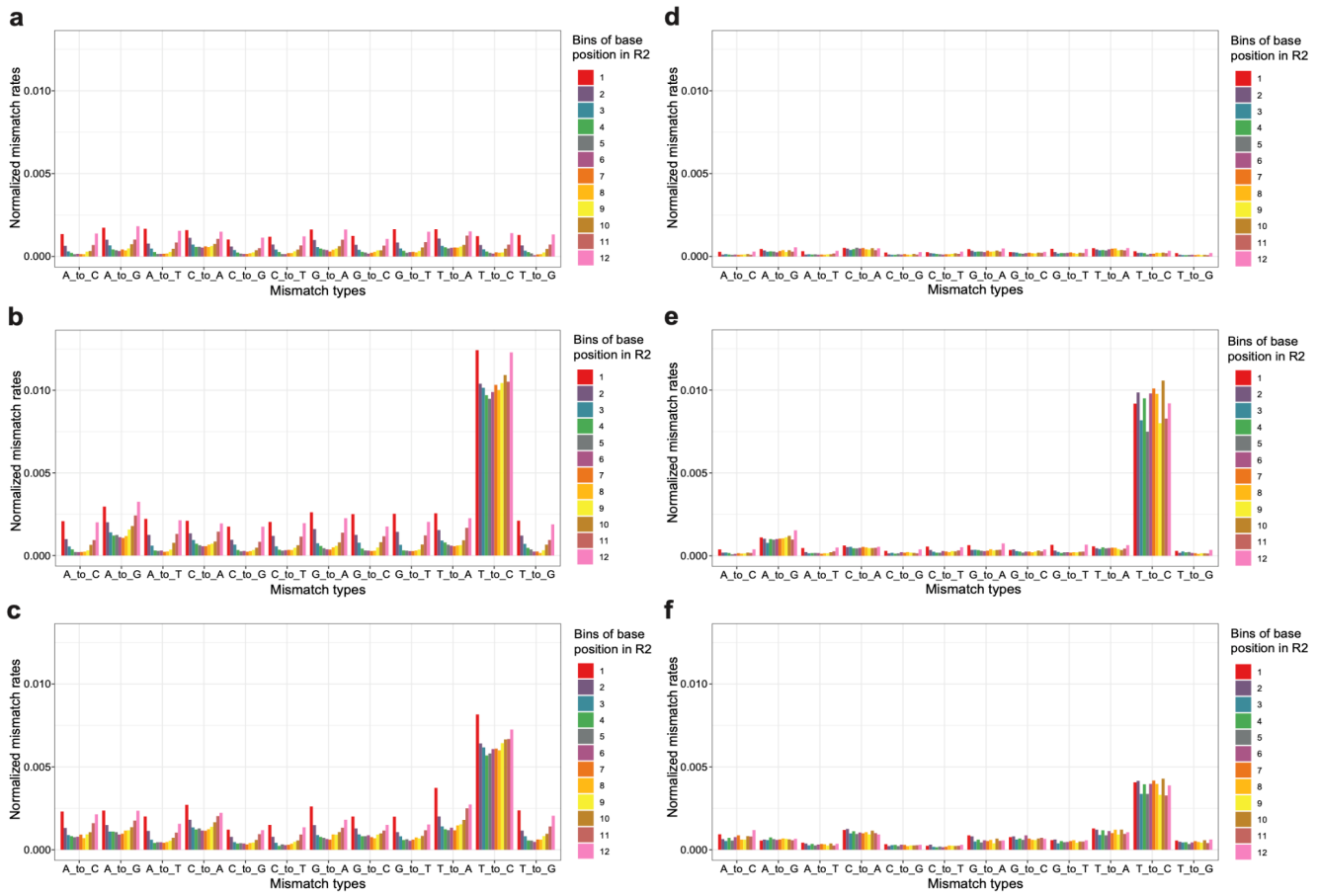

Extended Data Fig. 4. Optimization of the computational pipeline for nascent reads calling. a-c. Bar plots showing the normalized mismatch rates of all 12 mismatch types detected in unconverted cells (a), converted cells (b), and the original sci-fate A549 dataset[14] (c) at different positions of the reads using the original sci-fate mutation calling pipeline[14]. **d-f.** Bar plots showing the normalized mismatch rates of all 12 mismatch types detected in unconverted cells (d), converted cells (e), and the original sci-fate A549 dataset[14] (f) at different positions of the reads using the updated mutation calling pipeline. Considering the different sequencing lengths between the present dataset and sci-fate, the Read2 from sci-fate were trimmed to the same length as the present dataset before processing. Compared to the original pipeline, the updated pipeline further filtered the mismatch based on the CIGAR string and only mismatches with "CIGAR = M" were kept. As shown in the result, this optimized pipeline efficiently removed the unaligned mismatches enriched at the 5' and 3' end of reads. Normalized mismatch rates in each bin, the percentage of each type of mismatch in all sequencing bases within the bin.

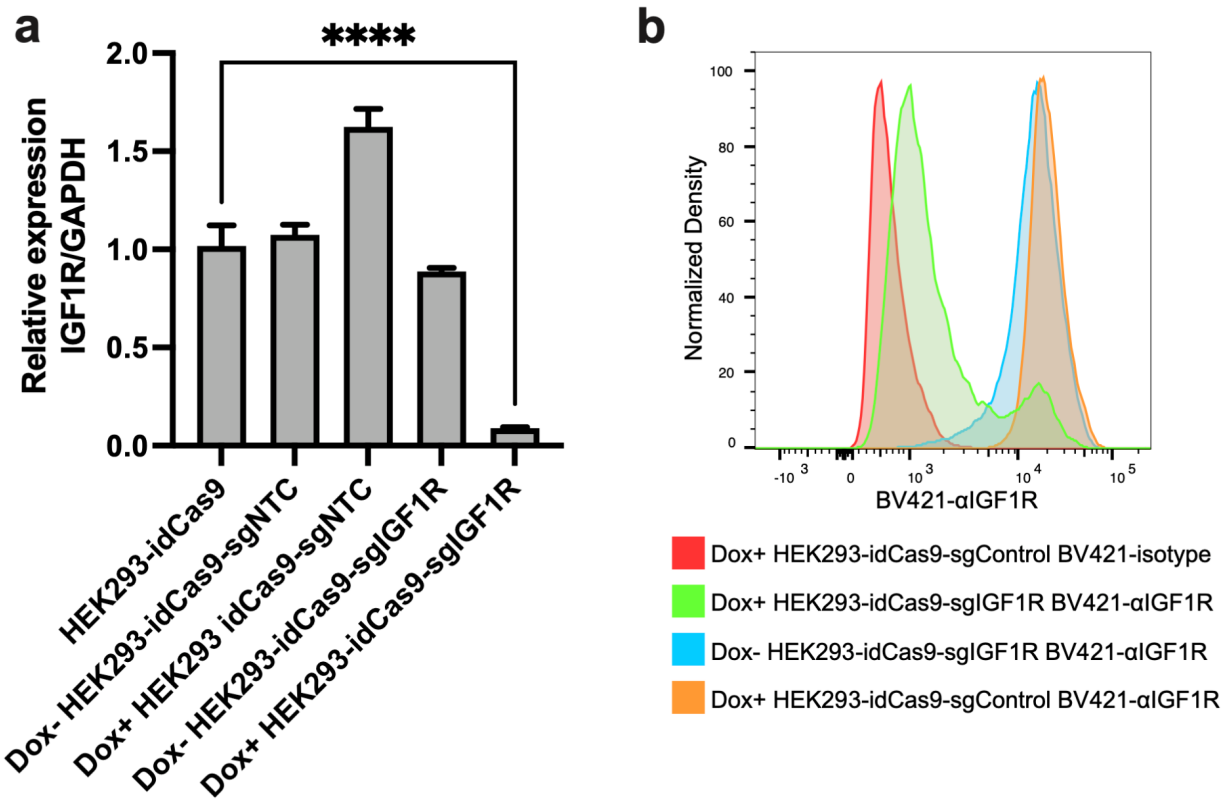

Extended Data Fig. 5. Validation of the CRISPRi performance. Strongly reduced *IGF-1R* mRNA and protein levels in HEK293-idCas9 cells after Dox induction were further validated by **a.** RT-qPCR (n=4. ****, p-value < 1e-4, Tukey's test after ANOVA) and **b.** flow cytometry. Isotype, isotype control. αIGFIR, anti-IGF1R.

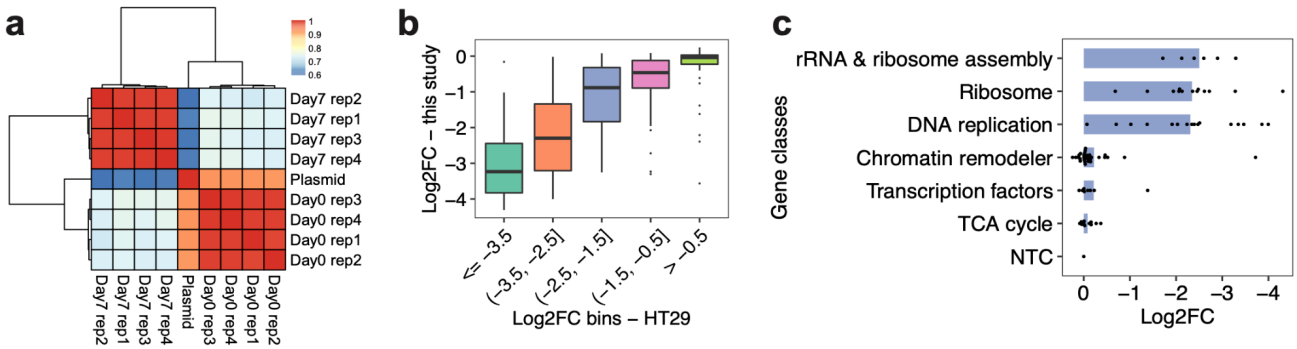

Extended Data Fig. 6. The changes in sgRNA abundance are consistent between replicates and previously published data. a. Heatmap showing the overall Pearson correlations of normalized sgRNA read counts between the plasmid library and bulk screen replicates at different sampling times. For each library, read counts of sgRNAs were normalized first by the sum of total counts and then by the counts of sgNTC. **b**. Box plot showing the reproducible trends of deletion upon CRISPRi between the present study and a prior report[29]. We calculated the fraction changes (After vs. before the CRISPRi induction) of sgRNAs for each gene, followed by log2 transformation. **c**. Bar plot showing the different extent of deletion of cells receiving sgRNAs targeting genes in different categories in the bulk screen. The knockdown on genes with higher essentiality caused stronger cell growth arrest.

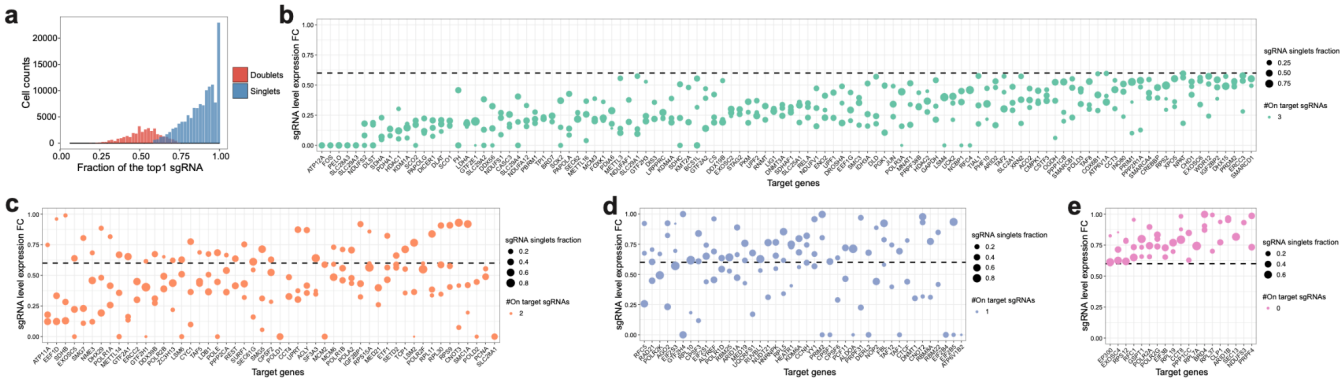

Extended Data Fig. 7. Quality control and sgRNA filtering on the *PerturbSci-Kinetics* library. a. We filtered out cells assigned to multiple gRNAs based on two criteria: the cell is defined as a sgRNA singlet if the most abundant sgRNA in the cell took >= 60% of total sgRNA counts and was at least 3-fold of the second most abundant sgRNA. The histogram shows the fraction distribution of the most abundant sgRNA in assigned singlets (78%) and doublet cells (22%). **b-e**. Dotplots showing the expression fold changes of target genes upon CRISPRi induction compared to NTC. Each dot represents a sgRNA. Fold change < 0.6 was used for sgRNA filtering, and target genes with 3, 2, 1, 0 on-target sgRNA(s) were shown in b-e, respectively. FC, fold change.

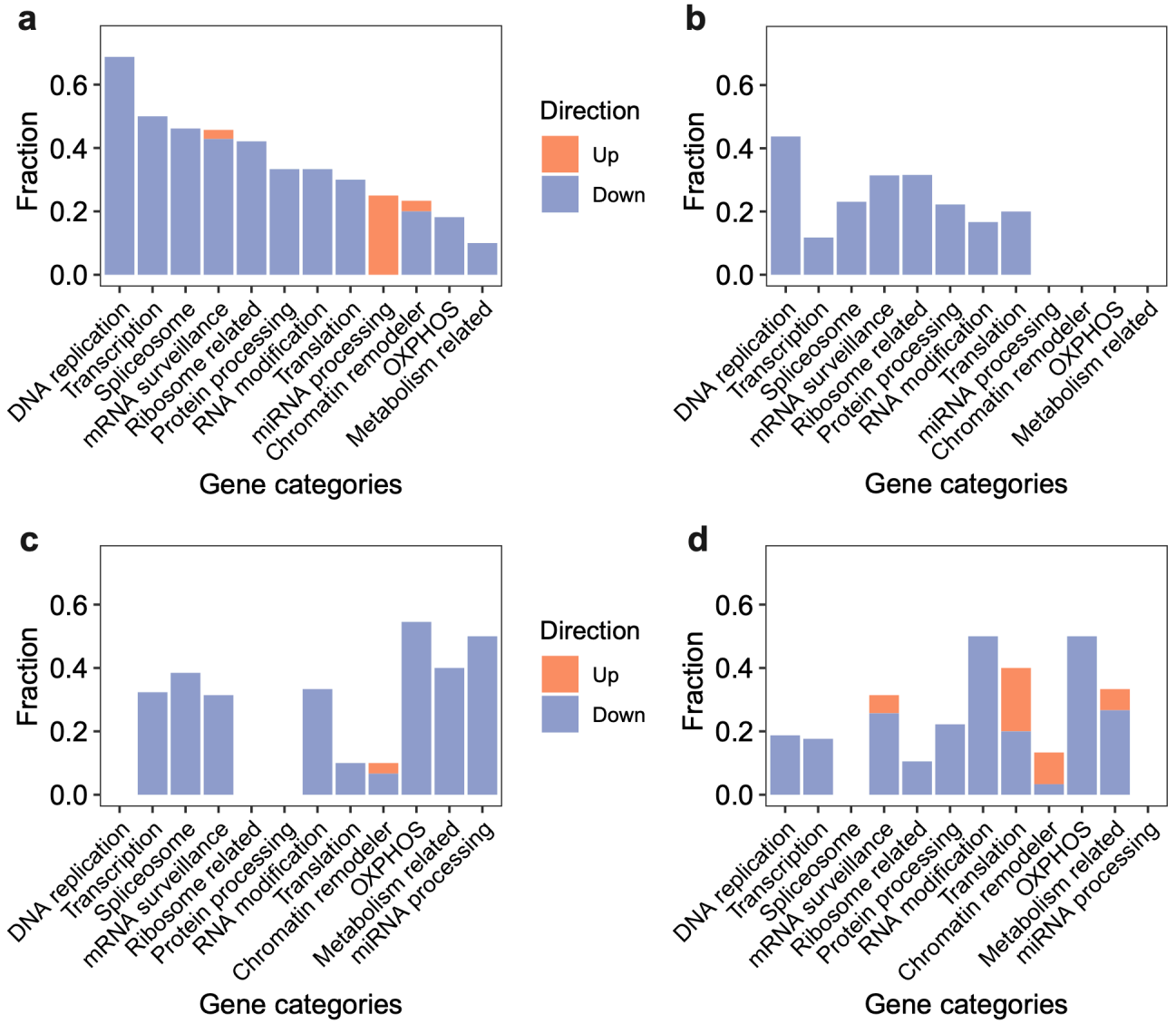

Extended Data Fig. 8. A systematic view of the effects of perturbations on global synthesis rates, global degradation rates, exonic reads ratio, and mitochondrial turnover rates. For each gene category, we calculated the fraction of genetic perturbations associated with significant changes in global synthesis rates (a), global degradation rates (b), fractions of exonic reads in the nascent transcriptome (c), and mitochondrial RNA turnover rates (d). Overall global transcription could be affected by more genes than degradation. Perturbation on essential genes, such as DNA replication genes, could affect both global synthesis and degradation. Perturbations on chromatin remodelers only specifically impaired the global synthesis rates but not the degradation rates, supporting the established theory that gene expression is

regulated by chromatin folding. In addition to the enrichment of genes in transcription, spliceosome and mRNA surveillance, perturbation on OXPHOS genes and metabolism-related genes also affected the RNA processing, consistent with the fact that 5' capping, 3' polyadenylation, and RNA splicing are highly energy-dependent processes. That knockdown of OXPHOS genes and metabolism-related genes could reduce the mitochondrial transcriptome dynamics and also supported the complex feedback mechanisms between energy metabolism and mitochondrial transcription[55].

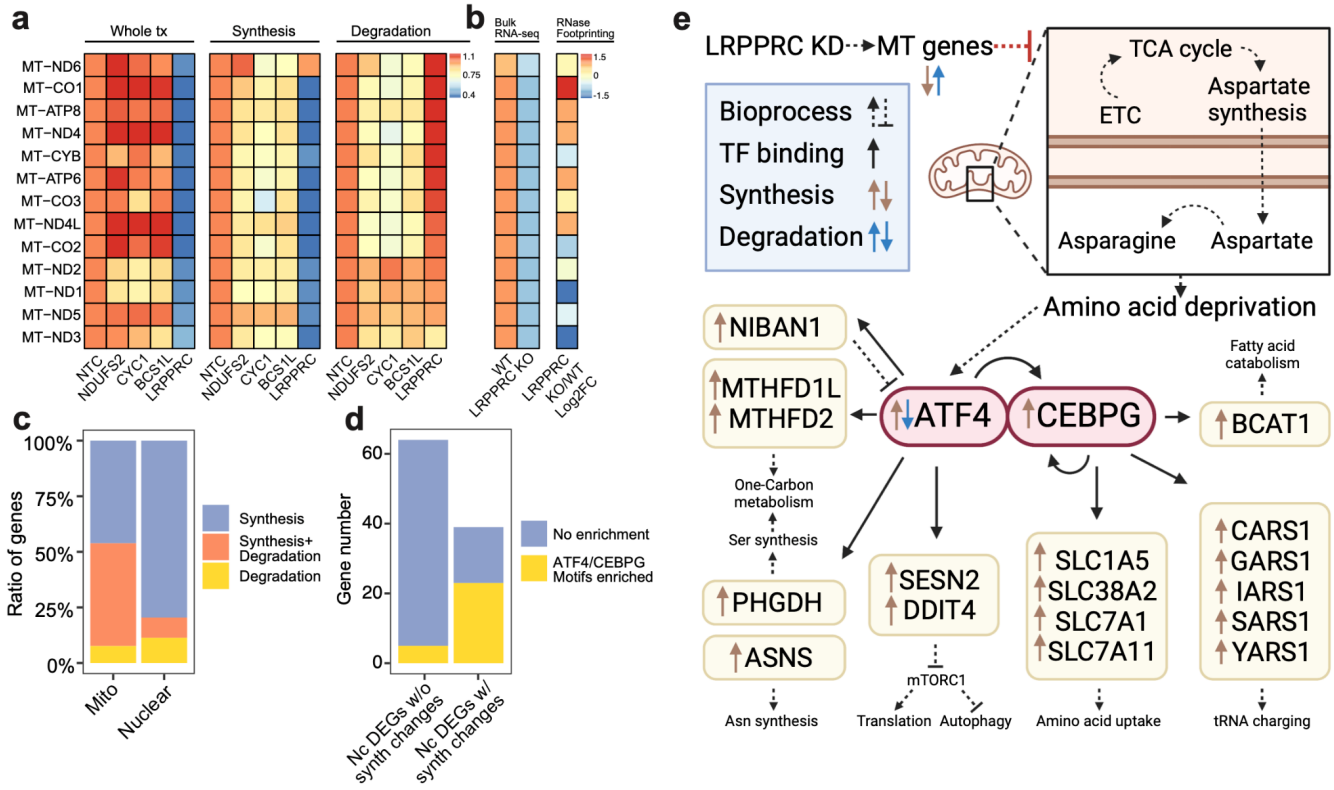

Extended Data Fig. 9. *PerturbSci-kinetics* identified LRPPRC as the master regulator of mitochondrial RNA dynamics. a. Heatmap showing the relative fold changes of gene expression, synthesis and degradation rates of mitochondrial protein-coding genes upon NDUFS2, CYC1, BCS1L and LRPPRC knockdown compared to NTC cells. Perturbation on genes encoding electron transport chain components resulted in stable steady-state expression with impaired turnover. However, LRPPRC knockdown significantly disrupted the mitochondrial transcriptome dynamics by inhibiting the synthesis of almost all mitochondrial protein-coding genes and promoting the degradation of multiple genes including *MT-ND6, MT-CO1, MT-ATP8, MT-ND4, MT-CYB* and *MT-ATP6*. **b.** The heatmap on the left showed the mitochondrial protein-coding gene expression changes between wild-type and *LRPPRC*-knockout mice heart tissue, as reported by Siira, S.J., et al. [37]. The heatmap on the right showed the extent of the mRNA secondary structure increase upon *Lrpprc* knockdown observed in the published study[37], which positively correlated with the elevated degradation rates of genes detected in our study (Pearson correlation r = 0.708, p-value = 6.8e-3). The result further validated the mRNA-stabilizing mechanism of *Lrpprc*. **c.** Bar plot showing the fraction of genes regulated by synthesis, degradation or both in mitochondrial-encoded and nuclear-encoded DEGs. **d.** Bar plot showing the enrichment of *ATF4/CEBPG*

motifs at promoter regions of DEGs with or without significant synthesis changes. Nc DEGs w/o synth changes, Nuclear-encoded differentially expressed genes without synthesis changes. Nc DEGs w/ synth changes, Nuclear-encoded differentially expressed genes with synthesis changes. A large part of synthesis-regulated nuclear-encoded DEGs showed motif enrichment, suggesting the activation of an integrated stress response transcriptional program mediated by ATF4/CEBPG upon LRPPRC knockdown[41]. 5kb regions around transcription start sites of input genes were used for motif scanning and enrichment calculation using RcisTarget[56]. We identified two transcription factors (*ATF4* and *CEBPG*) that were i) significantly upregulated upon *LRPPRC* knockdown ii) significantly over-represented in the surroundings of the transcription start site of the synthesis-regulated nuclear-encoded DEGs (Normalized motif enrichment score of 16 for *ATF4* and 16.6 for *CEBPG*). **e.** The transcriptional regulatory network in *LRPPRC* perturbation inferred from our analysis. Notably, it was consistent with the prior study[41] that *ATF4* was regulated at both transcriptional and post-transcriptional levels.

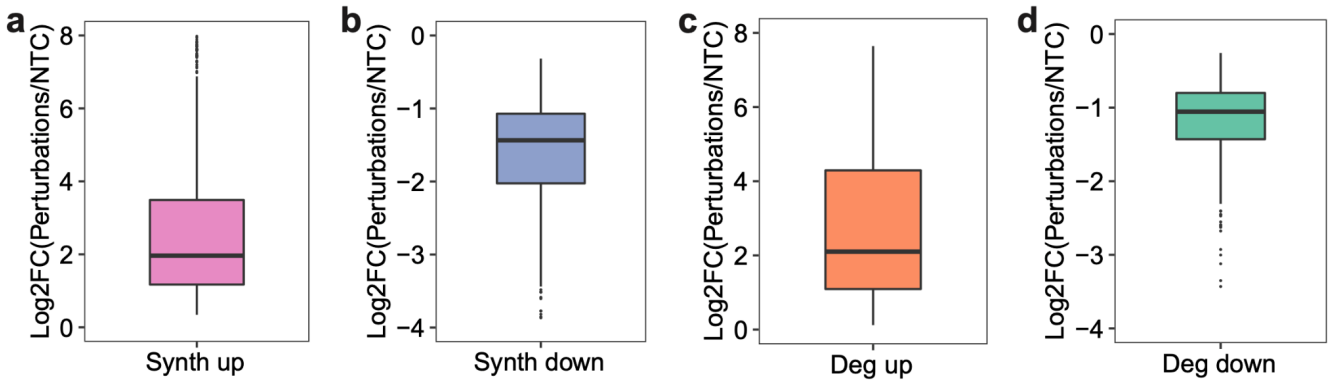

Extended Data Fig. 10. *PerturbSci-Kinetics* captured the synthesis/degradation rates of DEGs upon perturbations. a-d. Box plots showing the log2 transformed fold changes of synthesis or degradation rates between perturbations and NTC cells for DE genes in four categories: synth up (DEGs with significantly increased synthesis rates), synth down (DEGs with significantly decreased synthesis rates), deg up (DEGs with significantly increased degradation rates), deg down (DEGs with significantly decreased degradation rates).

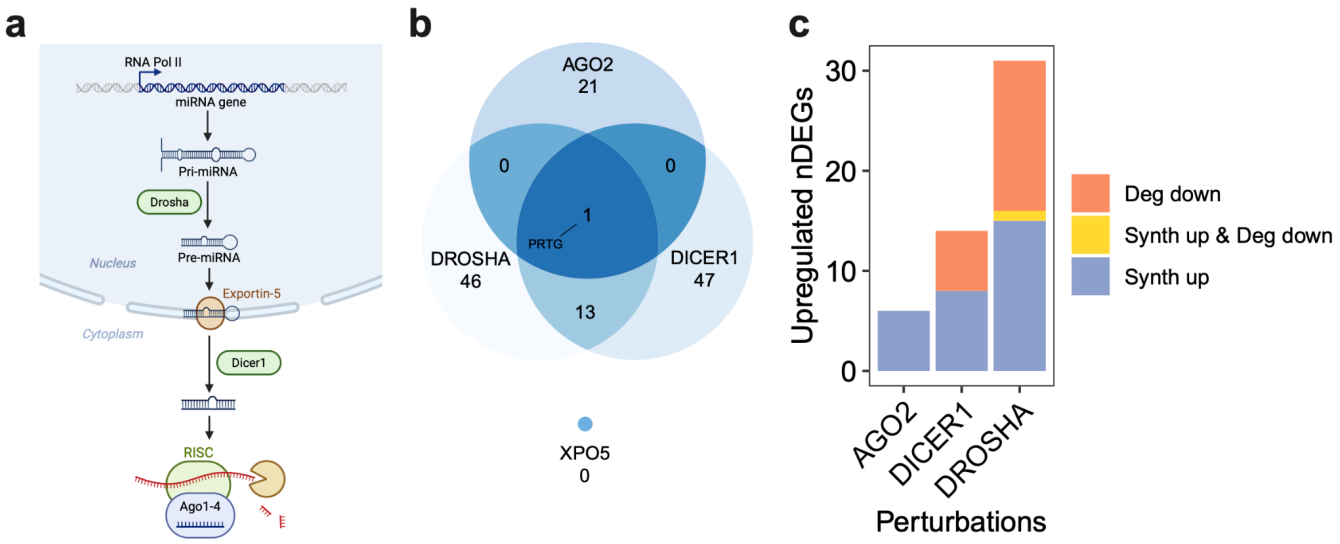

Extended Data Fig. 11. The overview of the miRNA biogenesis pathway and perturbations on pathway members. a. Illustration of the canonical miRNA biogenesis pathway. After the transcription of miRNA host genes, the primary miRNA (pri-miRNA) forms into a hairpin and is processed by *Drosha*. Processed precursor miRNA (pre-miRNA) is transported to the cytoplasm by Exportin-5. The stem loop is cleaved by *Dicer1*, and one strand of the double-stranded short RNA is selected and loaded into the RISC for targeting mRNA[44]. **b.** Venn diagram showing the overlap of upregulated DEGs across perturbations on four genes encoding main members of the miRNA pathway. The knockdown of two critical RNases in this pathway (*i.e., DROSHA* and *DICER1*) resulted in significantly overlapped DEGs (p-value = 2.2e-16, Fisher's exact test). In contrast, *AGO2* knockdown resulted in more unique transcriptome features, and only 1 DEG (*PRTG*, identified to be mainly regulated by degradation and has been reported as a miRNA target[57]) overlapped with DEGs from *DROSHA* and *DICER1* knockdown, indicating the RNAi-independent roles of *AGO2*. Interestingly, *XPO5* knockdown showed no upregulated DEGs, which is consistent with a previous report in which *XPO5* silencing only minimally perturbed the miRNA biogenesis, indicating the existence of an alternative miRNA transportation pathway[45]. **c.** Bar plot showing the fraction of upregulated DEGs driven by synthesis changes and degradation changes upon *DROSHA*, *DICER1*, and *AGO2* perturbations. While *DROSHA* and *DICER1* knockdown resulted in increased synthesis and reduced degradation, *AGO2* knockdown only affected gene expression transcriptionally, which was consistent with the previous finding that *AGO2* knockdown resulted in a global increase of synthesis rates **(Fig 2e)**, and further supported its roles in nuclear transcription regulation[58–60]. As *Drosha* is upstream of *Dicer1* in the pathway, we indeed observed stronger effects of *DROSHA* knockdown than *DICER1* knockdown, which was supported by the previous study[45].

Supplementary Tables (provided as Microsoft Excel files)

Supplementary Table 1: Genes and sgRNAs included in the study. Each gene ("gene_symbol") has 3 sgRNAs, and they were named in the format "Gene_number" ("names"). sgRNA sequences were included in "sgRNA_seq". The "gene_class" is the functional category of each gene.

Supplementary Table 2: Raw sgRNA counts of the bulk screen samples collected at different time points. Read counts of each sgRNA ("sgRNA_name") from 4 replicates at day 0 and day 7 were included.

Supplementary Table 3: Relative sgRNA abundance fold changes between day 7 and day 0. The "Day7_vs_Day0_repX" is the fold changes of relative sgRNA abundance at the gene level (**Methods**).

Supplementary Table 4: Filtered differentially expressed genes between perturbations with cell number >= 50 and NTC. For each gene ("Gene_symbol"), the "perturbation" is the target gene in perturbed cells. The "DEGs_direction" is the direction of gene expression changes comparing perturbed cells to the NTC cells, and the "DEGs_FC" is the fold change of the gene expression changes comparing perturbed cells to the NTC cells. The "max.CPM.between.KD.NTC" and "min.CPM.between.KD.NTC" are the pseudobulk expression levels of the gene that showed higher and lower expression in perturbed cells or the NTC cells. The expression level was quantified by counts per million. The "qval" is the false discovery rate (one-sided likelihood ratio test with adjustment for multiple comparisons).

Supplementary Table 5: Information about perturbations that showed significant global synthesis rate changes. The "adj.p" is the false discovery rate adjusted for multiple comparisons. The "direction" is the direction of the changes on the global synthesis rates distributions comparing perturbed cells to the NTC cells, and the "KD_median/NTC_median" is the quantitative measurement of the changes. The "gene_class" is the functional category of target genes ("Perturbations").

Supplementary Table 6: Information about perturbations that showed significant global degradation rate changes. The "adj.p" is the false discovery rate adjusted for multiple comparisons. The "direction" is the direction of the changes on the global degradation rates distributions comparing perturbed cells to the

NTC cells, and the "KD_median/NTC_median" is the quantitative measurement of the changes. The "gene_class" is the functional category of target genes ("Perturbations").

Supplementary Table 7: Information about perturbations that showed significant nascent exonic reads ratio changes. The "adj.p" is the false discovery rate adjusted for multiple comparisons. The "direction" is the direction of the changes on the nascent exonic reads ratio distributions comparing perturbed cells to the NTC cells, and the "KD_median/NTC_median" is the quantitative measurement of the changes. The "gene_class" is the functional category of target genes ("Perturbations").

Supplementary Table 8: Information about perturbations that showed significant mitochondrial RNA turnover changes. The "adj.p" is the false discovery rate adjusted for multiple comparisons. The "direction" is the direction of the changes in the distributions of mitochondrial nascent/total reads ratio comparing perturbed cells to the NTC cells, and the "KD_median/NTC_median" is the quantitative measurement of the changes. The "gene_class" is the functional category of target genes ("Perturbations").

Supplementary Table 9: Steady-state expression and synthesis/degradation dynamics of mitochondrial genes upon *LRPPRC*, *NDUFS2*, *CYC1*, *BCS1L* perturbations. The "synth_rate", "synth_FC", "synth_pval", "synth_direction" are the synthesis rate of the gene in the perturbed cells, the fold change of the synthesis rate of the gene in the perturbed cells compared to the NTC cells, the significance of the synthesis rate change, and the direction of the synthesis rate changes. The "deg_rate", "deg_FC", "deg_pval", "deg_direction" are the degradation rate of the gene in the perturbed cells, the fold change of the degradation rate of the gene in the perturbed cells compared to the NTC cells, the significance of the degradation rate change, and the direction of the degradation rate changes. The "DEG_qval" and "DEG_fold.change" are the multiple comparison-corrected FDR and the fold change of the steady-state gene expression change in perturbed cells compared to the NTC cells.

Supplementary Table 10: Differentially expressed genes with significant synthesis and/or degradation changes. The "perturbations" is the target gene of the perturbed cells, and the "Gene_symbols" is the symbols of DEGs with significant synthesis and/or degradation rate changes in corresponding perturbations. The type of significant rate change of each gene is included in the "Regulation_type". The "Synth_deg_FC", the "Synth_deg_direction", and the "Synth_deg_pval" reflect the fold change, the direction of the change, and the randomization test p-value of the rate indicated in the "Regulation_type".

"DEGs_FC", "DEGs_direction", and "max.expr.between.KD.NTC" are the fold changes of gene expression, the direction of the change, and the maximum pseudobulk CPM between the corresponding perturbation and the NTC cells.

Supplementary Table 11: Steady-state expression and synthesis/degradation dynamics of merged DEGs upon *DROSHA* and *DICER1* perturbations. The "synth_rate", "synth_FC", "synth_pval", "synth_direction" are the synthesis rate of the gene in the perturbed cells, the fold change of the synthesis rate of the gene in the perturbed cells compared to the NTC cells, the significance of the synthesis rate change, and the direction of the synthesis rate changes. The "deg_rate", "deg_FC", "deg_pval", "deg_direction" are the degradation rate of the gene in the perturbed cells, the fold change of the degradation rate of the gene in the perturbed cells compared to the NTC cells, the significance of the degradation rate change, and the direction of the degradation rate changes. The "DEG_fold.change" and "DEG_qval" are the fold change of the steady-state gene expression change in perturbed cells compared to the NTC cells and the multiple comparison-corrected FDR.

Supplementary files

Supplementary file 1: Detailed experiment protocols for *PerturbSci-Kinetics*, including all materials and equipment needed, step-by-step descriptions, and representative gel images.

Supplementary file 2: Primer sequences used in the *PerturbSci-Kinetics* experiment. The design principles and sequences of the oligo pool library, bulk screen sequencing primer, shortdT RT primers, sgRNA capture primers, ligation primers, sgRNA inner i7 primers, and P5/P7 primers were included. The columns indicate the positions on the 96-well plate (Well positions), an identifier of the sequence (Names), the full primer sequence (Sequences), and the barcode sequence (Barcodes).

Supplementary file 3: The overall costs for *PerturbSci-Kinetics* library preparation. Reagents used in each step were included, and the costs were calculated based on the scale of the real experiment.

Supplementary file 4: Computational pipeline scripts and notes for processing *PerturbSci-Kinetics* data, from sequencer-generated files to single-cell gene count matrix.